Chapter 2
Theory

2.1 Electrochemical Principles

Electrochemical cells are based on two half-cells, each having an electrode in contact with an electrolyte, joined electronically by external wires and ionically in the electrolyte phase in order to close the circuit. Fuel cells [1] and batteries [2] are two common types of electrochemical cells that are designed to convert chemical energy into electrical energy through electrochemical reactions at their two electrodes. In a fuel cell, which is a thermodynamically open process, a flow of externally stored fuel and oxidant is continuously supplied to the electrochemical cell to generate electrical power, in contrast to batteries where reactants and products are stored internally in a closed system without mass flux across its boundaries. A redox flow battery (RFB) [3] is an interesting device in this context, as it can be considered either a battery or a fuel cell depending on where the system boundaries are drawn. RFBs have independent energy conversion and energy storage subsystems similar to fuel cells but are generally categorized as batteries due to storage of charge within a closed liquid electrolyte system.

Both fuel cells and batteries principally comprise an anode and a cathode separated by an electrolyte, as shown schematically in Fig. 2.1 in the case of a fuel cell. The power generation function of electrochemical cells is conceptually straightforward. The fuel (or anodic reactant) is oxidized at the anode, releasing reaction products including ions and electrons. The ions travel through the electrolyte phase, which can be either a liquid or a polymer that promotes ionic conduction while insulating for electronic transport, and recombine with the oxidant (or cathodic reactant) at the cathode. The electrons required for the reduction reaction at the cathode are conducted from the anode through external wiring, thereby generating an electrical current used to drive a load. Fuel cell electrodes require contact between three separate phases at the active sites to facilitate heterogeneous electrochemical reactions that produce a useful current: the solid phase that conducts electrons to or from the electrode; the liquid or gaseous fuel or oxidant phase; and the liquid or solid polymeric electrolyte phase. In the case of a RFB, each reactant is in the liquid

E. Kjeang, *Microfluidic Fuel Cells and Batteries*, SpringerBriefs in Energy,
DOI 10.1007/978-3-319-06346-1_2, © The Author(s) - SpringerBriefs 2014

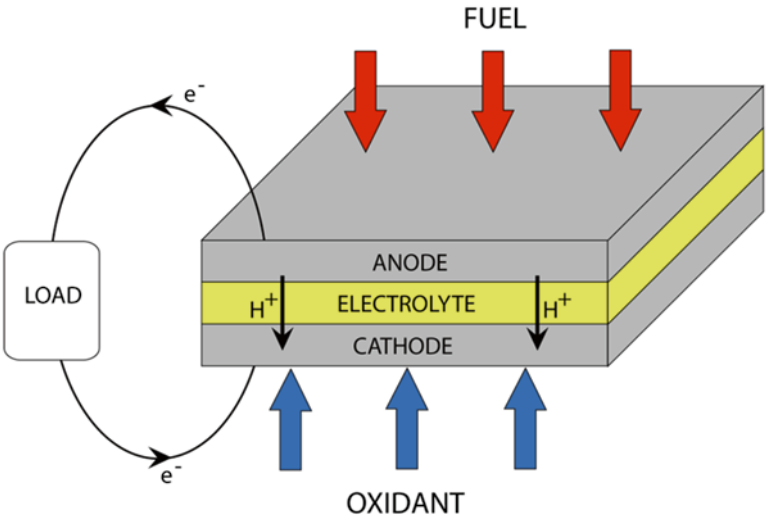

Fig. 2.1 Conceptual fuel cell layout showing the core components of the membrane electrode assembly (MEA): anode and cathode separated by a polymeric ion-conducting electrolyte and connected to an external load

phase in three-phase contact with a solid electrode and an ion-conducting liquid or polymeric electrolyte; however, the liquid reactant phase may contain supporting electrolyte to assist with ionic transport and thereby reduce the electrochemical interface to a pure solid–liquid interface. Although the electrochemical reactions are typically exothermic and therefore release energy, the reaction rates are often constrained by large activation energy that needs to be supplied for the reactions to proceed. There are three prevalent strategies to accelerate electrochemical reaction rates: (1) adding catalysts; (2) elevating the operating temperature; and (3) increasing the effective electrode area by incorporating micro- or nanostructured materials. The first two can be applied to any chemical reactions, while the third strategy is especially important in electrochemical cells due to the surface-based reactions that benefit from a high surface-to-volume ratio. Carbon-supported platinum (Pt/C) is widely utilized as electrocatalyst in low-temperature fuel cells, in particular for hydrogen and oxygen, due to its high activity. For other fuels such as formic acid and methanol, palladium, ruthenium, or various platinum alloys provide good catalytic properties. In contrast, most redox flow batteries benefit from rapid electrochemical kinetics on common carbon or graphite electrodes without any specific catalyst requirements.

The performance of electrochemical cells is normally measured in terms of cell voltage (ΔE_{cell}) and current (I). The cell voltage represents the difference in electrochemical potential between the two half-cells (cathode and anode), with a maximum at the reversible open-circuit voltage ($E_{\text{cathode}} - E_{\text{anode}}$). The reversible potential

of each electrode is determined from the Gibbs' free energy of the reactants and products at their standard states via the Nernst equation:

$$E = E^0 - \frac{RT}{F} \ln \frac{\coprod_{\text{products},i} a_i^{\upsilon_i}}{\coprod_{\text{reactants},j} a_j^{\upsilon_j}}, \tag{2.1}$$

where E^0 is the reversible potential at standard state, R is the universal gas constant, T is the temperature, F is Faraday's constant, and a is the activity of each species ($a = 1$ at standard state), which for gaseous and aqueous species can be approximated by the partial pressure and concentration, respectively. The actual cell voltage obtained during operation is significantly lower than the reversible cell potential due to various losses (also referred to as overpotentials). The operational cell voltage is determined by [1]:

$$\Delta E_{\text{cell}} = \left(E_{\text{cathode}} - E_{\text{anode}}\right) - \left|\eta_{\text{anode}}\right| - \left|\eta_{\text{cathode}}\right| - iR_{\text{cell}} - \eta_{\text{trans}} \tag{2.2}$$

where the subtracted terms correspond to voltage losses caused by activation overpotentials due to irreversibilities at the electrodes (η), ohmic resistance of the cell (R_{cell}), and concentration overpotentials from mass transport limitations (η_{trans}). The current density (i) is the cell current divided by the geometrical surface area of the electrode. Power density (mW cm^{-2}), which is an overall measure of the device level performance, is obtained by multiplying cell voltage and current density. The electrochemical reactions and electrode materials employed in microfluidic cells are generally consistent with those of conventional electrochemical cells, and the large body of literature available on electrochemistry can be adopted for detailed descriptions of applicable reaction mechanisms, kinetics, and overpotentials [4].

2.2 Fluid Dynamics

Microfluidics is the principal subject of fluid flow on the microscale and has been described as both a science and a technology [5, 6]. It is formally defined as the study and application of fluid flow and transport phenomena in microstructures with at least one characteristic dimension in the range of 1–1,000 μm [5, 6]. The subject of microfluidics regularly involves engineering, chemistry, and biology disciplines and serves a wide range of applications including lab-on-chip technologies, biomedical diagnostics, drug discovery, proteomics, and energy conversion. Squires and Quake [7] and Gad-El-Hak [8] provide comprehensive reviews of the physics of microfluidics. Fluid flow in microscale conduits is laminar under most conditions. Flow in this regime is characterized by low Reynolds' numbers $Re = \rho U D_h/\mu$, where ρ is the fluid density, U is the average velocity, D_h is the hydraulic diameter, and μ is the dynamic viscosity. Microfluidic laminar flow is dominated by viscous effects over inertial effects, and surface forces play a dominant role over body forces.

Microfluidic electrochemical cells exploit the properties of laminar flow in microchannels to delay convective mixing of two stratified streams carrying the respective anodic and cathodic reactants. At low *Re*, the two streams will flow in parallel down a single microfluidic channel, as shown schematically in Fig. 1.1. This type of flow is referred to as co-laminar flow and is functional in the laminar internal flow regime for *Re* up to approximately 1,000. Internal flows exceeding this threshold will transition to turbulence and destabilize the co-laminar flow interface, leading to excessive mixing and loss of cell voltage.

Due to the laminar nature of microfluidics, the velocity field $\overline{u}$ for incompressible Newtonian fluids is governed by the Navier–Stokes equations for momentum conservation in 3-D:

$$\rho\left(\frac{\partial \overline{u}}{\partial t}+\overline{u}\cdot\nabla\overline{u}\right)=-\nabla p+\mu\nabla^2\overline{u}+\overline{f}, \tag{2.3}$$

where p represents pressure and $\overline{f}$ summarizes the body forces per unit volume. The use of the Navier–Stokes equations assumes that the fluid may be treated as a continuum; however, this assumption is generally valid in microscale liquid flows [6–8] and may be applied with reasonable accuracy into the nanofluidic range. At very low *Re*, the nonlinear convective terms in the Navier–Stokes equations may be safely neglected, resulting in linear and predictable Stokes flow:

$$\rho\frac{\partial \overline{u}}{\partial t}=-\nabla p+\mu\nabla^2\overline{u}+\overline{f}. \tag{2.4}$$

Furthermore, mass conservation for fluid flow obeys the continuity equation:

$$\frac{\partial \rho}{\partial t}+\nabla\cdot\left(\rho\overline{u}\right)=0. \tag{2.5}$$

For fluids with constant density, this equation is reduced to the incompressibility condition, $\nabla\cdot\overline{u}=0$. In classical fluid dynamics problems, e.g., flow between parallel plates and flow in a cylindrical tube, Eqs. (2.4) and (2.5) lead to the familiar parabolic pressure-driven velocity profile, which serves as a useful baseline for microfluidics.

The surface-area-to-volume ratio, which is inversely proportional to the characteristic length, is comparatively high in microfluidic devices and increases with decreasing channel dimensions. A high surface-to-volume ratio is favorable for surface-based (i.e., heterogeneous) chemical reactions such as the electrochemical reactions occurring in fuel cells and batteries. However, reducing the size of the channel leads to increasing frictional losses and parasitic load required to drive the flow. It is hence important to consider the role of pressure drop due to friction when designing microfluidic electrochemical cells. The pressure drop required to generate a pressure-driven laminar flow with mean velocity U in a straight channel of length L and hydraulic diameter D_h is conveniently expressed as [9]

$$\Delta p=\frac{32\mu LU}{D_\mathrm{h}^2}. \tag{2.6}$$

The corresponding pumping power W required to drive the flow is obtained by multiplying the pressure drop with the flow rate Q:

$$W = \Delta pQ = \frac{32\mu LUQ}{D_{\mathrm{h}}^2}. \tag{2.7}$$

This relationship is valid for fully developed flow in a straight channel and does not include the contributions from inlet and outlet feed tubes and minor losses due to ports, bends, expansions/contractions, steps, corners, etc. In most microfluidic fuel cell designs, however, relatively long thin channels are applied where friction losses of the type described by Eq. (2.6) are known to dominate.

2.3 Transport Phenomena

Microfluidic laminar flows enable a great deal of control over fluid–fluid interfaces [10] and provide unique functionality. Most important for microfluidic electrochemical cells is co-laminar streaming. Specifically, when two liquid streams of similar fluids in terms of viscosity and density are joined in a single microfluidic channel, a parallel co-laminar flow is established. The resulting fluid–fluid interface may be applied to observe chemical reactions in real time, serve as a lens, or separate reactants as required for microfluidic electrochemical cells. Species transport within microscale flows can occur through convection, diffusion, and electromigration. In the absence of electromigration, mixing between two co-laminar streams occurs by crosswise diffusion alone. Microscale devices generally experience high Péclet numbers $Pe = UD_{\mathrm{h}}/D$, where D is the diffusion coefficient. High Péclet numbers indicate that the rate of mass transfer via crosswise diffusion is much lower than the streamwise convective velocity. In the case of microfluidic electrochemical cells, diffusive mixing is therefore restricted to a thin interfacial width at the center of the channel. This interfacial mixing width has an hourglass shape with maximum width (δ_x) at the channel walls as described by the following scaling law [11] for pressure-driven laminar flow of two aqueous solutions:

$$\delta_x \propto \left(\frac{DHz}{U}\right)^{1/3}, \tag{2.8}$$

where z is the downstream position and H is the channel height. Eq. (2.8) is limited, however, to liquids of similar density. With disparate densities, a gravity-induced reorientation of the co-laminar liquid–liquid interface can occur [12]. The physics of co-laminar flow is the key-enabling mechanism of several microfluidic devices such as the T-sensor [13], Y-mixer [14], and H-filters [15] with applications in lab-on-chip diagnostic technologies and can also be applied to selectively pattern microfluidic systems [16].

Microfluidic electrochemical cells, as shown in Fig. 1.1, employ one laminar stream that contains the fuel (or first reactant) and a second laminar stream that contains the oxidant (or second reactant). As the fuel and oxidant streams flow in a

co-laminar format, the liquid–liquid interface serves as a virtual separator without the need for a membrane. The positions of the electrodes on the channel walls are however constrained by the width of the co-laminar interdiffusion zone. To prevent mixed potentials due to fuel and oxidant crossover, the electrodes must have sufficient separation from the liquid–liquid interface throughout the channel. The position and orientation of the electrodes also influence fuel utilization and overall performance of the cell. Notably however, the degree of mixing in microfluidic electrochemical cells can be effectively controlled by tuning the flow rate in the channel, vis-à-vis Eq. (2.8). Specifically, the residence time t_{res} in the electrochemical chamber must be shorter than the diffusion time t_{diff} for crossover of a reactant species to the opposite electrode in order to avoid a mixed electrode potential. This necessary criterion can be estimated using Einstein's relation for one-dimensional Brownian diffusion [17], which provides a lower bound on the average diffusion time:

$$t_{res} = \frac{L}{U} < \frac{W^2}{2D} = \overline{t_{diff}}. \tag{2.9}$$

This equation includes two channel size parameters, namely the channel length L and width W (the mean diffusion distance). The mean velocity is determined by dividing the flow rate Q by the channel height H and width W. These additional constraints can be included to obtain a useful dimensionless relation for the ratio of solute (reactant) advection to cross-stream diffusion in co-laminar flow cells:

$$\frac{QW}{2DHL} > 1. \tag{2.10}$$

A similar design rule can also be derived for this geometry from the Péclet number [18], which is the ratio between advective flux and diffusive flux. From this point of view, Eq. (2.10) is satisfied when the rate of downstream advective transport exceeds the rate of reactant crossover towards the opposite electrode. As the relation is derived for an average diffusion time, it is recommended for the ratio to exceed 1 by an appreciable margin. For instance, to accommodate a suggested minimum ratio of 10 for a species with a ~10^{-10} m^2 s^{-1} diffusion coefficient in a 0.5 mm high, 0.5 mm wide, and 10 mm long channel, the required flow rate is on the order of ~1 μL min^{-1}.

Both co-laminar streams must have relatively high ionic conductivity to facilitate good ionic charge transport between the electrodes and to close the electrical circuit. High conductivity is normally provided by the addition of a supporting electrolyte that contains ions with high mobility, e.g., hydronium or hydroxide ions. The supporting electrolyte also stabilizes the co-laminar flow with respect to electromigration of fuel and oxidant species, since it is these highly mobile constituents that redistribute and shield the effects of the electric field and electric double layers in the channel. The ohmic resistance for ionic transport in the channel can be expressed in terms of the average charge-transfer distance between the electrodes (d_{ct}), the cross-sectional area for charge transfer (A_{ct}), and the ionic conductivity (σ) as follows:

$$R_f = \frac{d_{ct}}{\sigma A_{ct}}. \tag{2.11}$$

Equation (2.11) indicates that a strong supporting electrolyte with high ionic conductivity and a high aspect ratio rectangular microchannel with closely spaced electrodes are therefore desired. This design strategy is partially in conflict with that required for efficient separation of fuel and oxidant. Principally, the interdiffusion width according to Eq. (2.8) indicates a lower limit on the electrode spacing. Striking an adequate balance between the competing requirements for species transport and ionic conductivity is essential in microfluidic electrochemical cells. Ohmic resistance in these cells is generally higher than in MEA-based fuel cells due to the additional constraints for cell design. Increasing the concentration of the supporting electrolyte is a convenient mitigation approach to achieve higher conductivity than for ionomer membranes. Ultimately, however, the choice of supporting electrolyte should be made with consideration of optimum reaction kinetics. The co-laminar configuration uniquely permits the composition of the two streams to be chosen independently, thus providing an opportunity to improve reaction rates and cell voltage. Similarly, the cell potential can be increased through adjusting the reversible half-cell potentials by pH modification of the individual streams.

Reactant transport from the bulk flow to the electrode surface takes place primarily by convection and diffusion in the absence of significant electromigration, provided a strong supporting electrolyte is used. In this case, species conservation takes the general form:

$$\nabla \cdot \left(C_i \overline{u} \right) = -\nabla \cdot \overline{J}_i + R_i, \tag{2.12}$$

where C_i is the local concentration of species i and R_i is a source term that describes the net rate of generation or consumption of species i via homogeneous chemical reactions. Under the infinite dilution assumption, the diffusive flux of species i is calculated by Fick's law:

$$\overline{J}_i = -D_i \nabla C_i \tag{2.13}$$

where D_i is the diffusion coefficient of the species i in the appropriate medium. Heterogeneous electrochemical reactions at the electrode surfaces are the boundary conditions of Eq. (2.13). The ratio of reaction rate and mass transport rate is defined by the Damköhler number (Da). When a current is drawn, a concentration boundary layer develops over the electrode starting at the leading edge. Assuming the electrochemical reactions are rapid (high Da), the maximum current density of a microfluidic electrochemical cell is determined by the rate of the convective/diffusive mass transport from the bulk to the surface of the electrode. In this transport limited case, the reactant concentration is zero at the entire surface of the electrode. Kjeang et al. [19] provided scaling laws for microfluidic fuel cell operation in the transport-controlled regime based on pseudo-3D flow over a flat plate, using previously developed theory for electrochemical flow sensors [20] originating from the classical Graetz problem of heat transfer [21]. The analysis is based on dimensionless formulations of mean velocity and current:

$$U^* = \frac{UD_h^2}{lD}, \tag{2.14}$$

$$I^* = \frac{I}{nFdlc_0 D / D_h}. \tag{2.15}$$

There are two distinct regimes: (1) the high U^* regime, which covers most practical flow rates experienced in microfluidic fuel cells and (2) the low U^* regime for low flow rates in channels with small hydraulic diameter. In the high U^* regime, the transport limited current is proportional to the cubic root of the mean velocity [20]:

$$I^* = -1.849U^{*1/3}. \tag{2.16}$$

In the low U^* regime, the flux of reactant entering the channel is equal to the rate of the electrochemical reactions, such that all reactant molecules are converted into product species and useful current. In this case, the maximum current is directly proportional to inlet concentration and flow rate [20]:

$$I = -nFc_0 Q. \tag{2.17}$$

Again, we can use the dimensionless quantities I^* and U^* to derive a relationship that is valid for high aspect ratio channels under any conditions within the low U^* regime:

$$I^* = -\frac{1}{2}U^*. \tag{2.18}$$

The transition point between the high U^* regime and the low U^* regime occurs at $U^{*1/3} = 1.9$ [20]. The coulombic single-pass fuel utilization can also be defined in this context as the rate of reactant consumption by the electrochemical reactions divided by the flux of reactant supplied by the flow:

$$\varepsilon_f = \frac{I}{nFc_0 Q}. \tag{2.19}$$

More generally, there is no single dominating limiting factor, and the current density of a microfluidic cell is controlled by a combination of mass transport, electrochemical kinetics, and ohmic resistance. This trio of potential limiting factors must be considered when designing a new device. The overall single-pass energy conversion efficiency of microfluidic electrochemical cells is defined by the product of the coulombic efficiency (fuel utilization) and voltage efficiency. In the case of galvanic cells, the energy conversion efficiency for discharging is written as

$$\varepsilon = \varepsilon_f \cdot \varepsilon_v = \frac{I}{nFc_0 Q} \cdot \frac{E_{\text{cell}}}{E^\circ_{\text{cell}}}, \tag{2.20}$$

where E_{cell}° represents the theoretical, reversible cell potential. This potential is sometimes replaced by the thermodynamic cell potential, E_{th}, to calculate the thermodynamic efficiency of a fuel cell. In the case of electrolytic cells, the voltage efficiency term is reversed, and the energy conversion efficiency for charging is given by

$$\varepsilon = \varepsilon_f \cdot \varepsilon_v = \frac{I}{nFc_0 Q} \cdot \frac{E^\circ_{\text{cell}}}{E_{\text{cell}}}. \tag{2.21}$$

This equation assumes that all applied current contributes to the desired electrolytic cell reaction; if parasitic side reactions are present that consume a portion of the applied current, such additional coulombic losses must also be accounted for in the coulombic efficiency.

In addition, the parasitic pumping power requirements to drive the flow (Eq. (2.7)) must be kept substantially below the power produced by the cell. In principle, any power consumption required for cell operation ought to be accounted for in the overall system efficiency of the device. Microchannels with ~μL to ~mL per minute flow rates generally provide an optimum balance with respect to the above-mentioned constraints.

References

1. J. Larminie, A. Dicks, *Fuel Cell Systems Explained* (Wiley, Hoboken, 2003)
2. R.M. Dell, D.A.J. Rand, *Understanding Batteries* (Royal Society of Chemistry, London, 2001)
3. D.P. de Leon, A. Frias-Ferrer, J. Gonzalez-Garcia, D.A. Szanto, F.C. Walsh, J. Power. Sources **160**, 716–732 (2006)
4. W.M. Haynes (ed.), *CRC Handbook of Chemistry and Physics*, 94th edn (Taylor & Francis/CRC Press, New York, 2013)
5. G.M. Whitesides, Nature **442**, 368–373 (2006)
6. N.T. Nguyen, S.T. Wereley, *Fundamentals and Applications of Microfluidics* (Artech House, Boston, MA., 2002)
7. T.M. Squires, S.R. Quake, Rev. Mod. Phys. **77**, 977–1026 (2005)
8. M. Gad-el-Hak, Phys. Fluids **17**, 100612 (2005)
9. C.T. Crowe, D.F. Elger, J.A. Roberson, *Engineering Fluid Mechanics* (Wiley, New York, 2001)
10. J. Atencia, D.J. Beebe, Nature **437**, 648–655 (2005)
11. R.F. Ismagilov, A.D. Stroock, P.J.A. Kenis, G. Whitesides, H.A. Stone, Appl. Phys. Lett. **76**, 2376–2378 (2000)
12. S.K. Yoon, M. Mitchell, E.R. Choban, P.J.A. Kenis, Lab Chip **5**, 1259–1263 (2005)
13. A.E. Kamholz, B.H. Weigl, B.A. Finlayson, P. Yager, Anal. Chem. **71**, 5340–5347 (1999)
14. J.B. Salmon, C. Dubrocq, P. Tabeling, S. Charier, D. Alcor, L. Jullien, F. Ferrage, Anal. Chem. **77**, 3417–3424 (2005)
15. J.P. Brody, P. Yager, Sensor. Actuator. Phys. **58**, 13–18 (1997)
16. P.J.A. Kenis, R.F. Ismagilov, G.M. Whitesides, Science **285**, 83–85 (1999)
17. A. Einstein, *Investigations on the Theory of the Brownian Movement*, vol. 17, 2nd edn. (Dover Publications, Mineola, NY, 1956)
18. R. Byron Bird, W.E. Stewart, E.N. Lightfoot, *Transport Phenomena*, 2nd edn. (Wiley, New York, 2001)
19. E. Kjeang, J. McKechnie, D. Sinton, N. Djilali, J. Power. Sources **168**, 379–390 (2007)
20. E. Kjeang, B. Roesch, J. McKechnie, D.A. Harrington, N. Djilali, D. Sinton, Microfluid. Nanofluid. **3**, 403–416 (2007)
21. L. Graetz, U¨ber die Wa¨rmeleitungsfa¨higkeit von Flu¨ssigkeiten. Ann. Physik. **25**, 337–357 (1885)

http://www.springer.com/978-3-319-06345-4

Microfluidic Fuel Cells and Batteries

Kjeang, E.

2014, X, 76 p. 17 illus. in color., Softcover
ISBN: 978-3-319-06345-4